Title
Human red and green cone opsins are O-glycosylated at an N-terminal Ser/Thr–rich domain conserved in vertebrates

Journal
Journal of Biological Chemistry, 294(20)

ISSN
0021-9258

Authors
Salom, David
Jin, Hui
Gerken, Thomas A
et al.

Publication Date
2019-05-01

DOI
10.1074/jbc.ra118.006835

Peer reviewed

Human red and green cone opsins are *O*-glycosylated at an N-terminal Ser/Thr–rich domain conserved in vertebrates

Received for publication, November 22, 2018, and in revised form, March 15, 2019 Published, Papers in Press, April 4, 2019, DOI 10.1074/jbc.RA118.006835

David Salom[‡§1], Hui Jin[§], Thomas A. Gerken[¶], Clinton Yu[‖], Lan Huang[‖], and Krzysztof Palczewski[‡§2]

From the [‡]Gavin Herbert Eye Institute and the Department of Ophthalmology, University of California, Irvine, Irvine, California 92697, the Departments of [§]Pharmacology and [¶]Biochemistry and Chemistry, Case Western Reserve University, Cleveland, Ohio 44106, and the [‖]Department of Physiology and Biophysics, University of California, Irvine, Irvine, California 92697

Edited by Henrik G. Dohlman

There are fundamental differences in the structures of outer segments between rod and cone photoreceptor cells in the vertebrate retina. Visual pigments are the only essential membrane proteins that differ between rod and cone outer segments, making it likely that they contribute to these structural differences. Human rhodopsin is *N*-glycosylated on Asn[2] and Asn[15], whereas human (h) red and green cone opsins (hOPSR and hOPSG, respectively) are *N*-glycosylated at Asn[34]. Here, utilizing a monoclonal antibody (7G8 mAB), we demonstrate that hOPSR and hOPSG from human retina also are *O*-glycosylated with full occupancy. We determined that 7G8 mAB recognizes the N-terminal sequence [21]DSTQSSIF[28] of hOPSR and hOPSG from extracts of human retina, but only after their *O*-glycans have been removed with *O*-glycosidase treatment, thus revealing this post-translational modification of red and green cone opsins. In addition, we show that hOPSR and hOPSG from human retina are recognized by jacalin, a lectin that binds to *O*-glycans, preferentially to Gal–GalNAc. Next, we confirmed the presence of *O*-glycans on OPSR and OPSG from several vertebrate species, including mammals, birds, and amphibians. Finally, the analysis of bovine OPSR by MS identified an *O*-glycan on Ser[22], a residue that is semi-conserved (Ser or Thr) among vertebrate OPSR and OPSG. These results suggest that *O*-glycosylation is a fundamental feature of red and green cone opsins, which may be relevant to their function or to cone cell development, and that differences in this post-translational modification also could contribute to the different morphologies of rod and cone photoreceptors.

Rod and cone photoreceptors are modified neurons evolved to detect and transduce light. Photoreceptor cells have an organelle, the outer segment (OS),[3] containing stacks of several hundred discs. The membrane protein composition of rod and cone OS discs is similar, except that each type of photoreceptor typically contains only one type of visual opsin that determines their spectral sensitivity. Because rhodopsin (and presumably cone opsins) accounts for ~50% of the area of the OS disc membranes (1), small structural differences between the visual opsins can have a profound impact on the overall structure of the photoreceptor. A second protein, the tetra-spanning membrane protein peripherin and, to some degree, its close relative the rod outer segment membrane protein 1 (ROM1) are also necessary for the formation and maintenance of OS (2). However, peripherin and ROM1 are identical in rod and cone OS, so they alone cannot account for the structural differences between photoreceptors.

Vision among mammals typically relies on three different visual opsins: blue and green/red cone opsins for color vision, and rhodopsin for low-illumination vision. However, humans (and closer primates) are capable of trichromatic vision due to a relatively recent duplication of the green/red cone opsin gene (3). Human green and red cone opsins (OPSG and OPSR, respectively) share 96% of sequence identity and are predicted to contain the same post-translational modifications (PTMs).

Rhodopsin is *N*-linked glycosylated at two N-terminal Asn residues. Although the role of this PTM is not fully understood, studies show that *N*-linked glycosylation of rhodopsin is necessary for its incorporation into the rod outer segment (ROS), morphogenesis and maintenance of ROS (4), and for the proper function of rhodopsin (5, 6). Less is known about the position and role of the *N*-glycans associated with cone opsins. Human cone opsins are predicted to be *N*-glycosylated at a single N-terminal residue. Experiments carried out with hOPSG heterologously expressed in insect Sf9 cells are consistent with *N*-glycosylation at Asn[34] (7, 8).

Another less-characterized PTM of proteins is mucin-type *O*-glycosylation (henceforth referred to as *O*-glycosylation), where glycans are attached to Ser/Thr residues via α-*N*-acetyl-

This work was supported in part by National Institutes of Health Grants EYR24024864 and R01EY027283 (to K. P.), R01GM113534 (to T. A. G.), and R01GM074830 and R01GM130144 (to L. H.), the Canadian Institute for Advanced Research (CIFAR), and the Alcon Research Institute (ARI). K. P. is CSO at Polgenix, Inc. The content is solely the responsibility of the authors and does not necessarily represent the official views of the National Institutes of Health.

This article contains Figs. S1–S6 and Tables S1 and S2.

[1] To whom correspondence may addressed. Tel.: 949-824-5154; E-mail: dsalom1@uci.edu.

[2] Holds the Leopold Chair of Ophthalmology. To whom correspondence may addressed: Gavin Herbert Eye Institute, Dept. of Ophthalmology, University of California, Irvine, Irvine, CA 92697. Tel.: 949-824-6527; E-mail: kpalczew@uci.edu.

[3] The abbreviations used are: OS, outer segment; 13LGS, 13-lined ground squirrel; AP, alkaline phosphatase; COS, cone outer segment; GPCR, G protein–coupled receptor; LMNG, lauryl maltose neopentyl glycol; OPSG, green cone opsin; OPSR, red cone opsin; PNGase F, peptide:*N*-glycosidase F; PTM, post-translational modification; PVDF, polyvinylidene fluoride; ROS, rod outer segment; EVP, enhancement value product; h, human; b, bovine; BisTris, 2-[bis(2-hydroxyethyl)amino]-2-(hydroxymethyl)propane-1,3-diol; mAB, monoclonal antibody; T4L, T4 lysozyme.

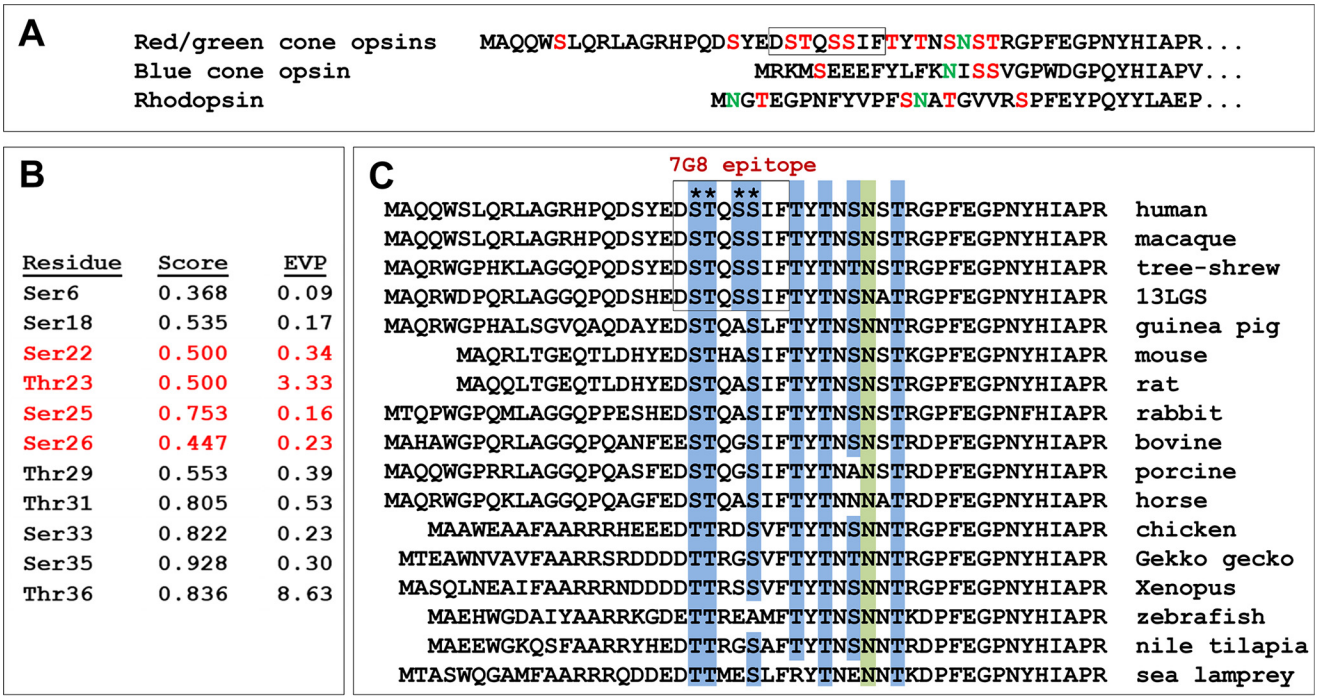

Figure 1. N termini of red/green cone opsins. *A,* N termini of human visual opsins. *Red* indicates Ser/Thr residues that potentially could be *O*-glycosylated. *Green* indicates *N*-glycosylated Asn residues. The epitope of the 7G8 mAB is *boxed*. *B,* NetOGlyc 4.0 score and ISOGlyP (beta2.1) *O*-glycosylation EVP results for human green cone opsin (NetOGly score values >0.5 and ISOGlyP EVP values >1.0 suggest possible glycosylation. See Table. S1 for the full ISOGlyP output.). Residues in *red* belong to the epitope of 7G8 mAB. The input in both cases was the full hOPSG sequence. *C,* conserved Ser/Thr residues at the N termini of vertebrate red/green cone opsins (highlighted in *blue*). The epitope of 7G8 mAB is in a *black box*. Human residues Ser^{22}, Thr^{23}, Ser^{25}, and Ser^{26} are marked with *asterisks*. *N*-Glycosylated Asn residues are highlighted in *green*.

galactosamine (GalNAc). This type of *O*-glycosylation is initiated by a family of ~20 GALNT glycosyltransferases that possess varying unique and overlapping peptide sequence preferences (9, 10); hence, the ability to predict such sites of *O*-glycosylation has been largely unsatisfactory. Furthermore, unlike peptide:*N*-glycosidase F (PNGase F) for *N*-glycans, *O*-glycosylation is difficult to study as there is not a single glycosidase able to remove all *O*-linked glycan structures. Understanding the key role of protein *O*-glycosylation is of biomedical importance because it is a common modification of proteins, and it is involved in biological functions and pathologies such as proprotein processing, ectodomain shedding, cell signaling, cell adhesion, and tumor formation (11). Several G protein–coupled receptors (GPCRs) from different families have been reported to be *O*-glycosylated, and it has been proposed that this PTM can modulate N-terminal cleavage and activity (11). In this investigation, we demonstrate that OPSR and OPSG in the retina of humans and several other vertebrates are *O*-glycosylated in a relatively homogeneous manner and with a full occupancy. Mass spectrometry (MS) analysis of bovine OPSR identified Ser^{22} as the *O*-glycosylation site, a residue that is semi-conserved (Ser or Thr) among vertebrates, suggesting an important role of *O*-glycosylation, perhaps in the unique features of green and red cone photoreceptors. In addition, our findings show that OPSG heterologously expressed in mammalian and insect cells is *O*-glycosylated but has a glycan pattern and/or occupancy that is different from that observed in retina, emphasizing that heterologous expression systems are often unable to mimic the PTMs observed in native tissues.

Results

O-Glycosylation of OPSR/OPSG in humans and other mammals

Visual opsins contain several PTMs at their N termini. Human rhodopsin is acetylated at Met^1 and *N*-glycosylated at Asn^2 and Asn^{15}, whereas human cone opsins are predicted to have one *N*-glycosylated Asn residue (8). We observed that the N terminus of hOPSR/hOPSG has an unusually high content of Ser/Thr residues (Fig. 1*A*), with most of them highly conserved in vertebrates (Fig. 1*C*). Most of these N-terminal Ser/Thr residues have a score equal to or higher than 0.5 using the NetOGlyc 4.0 Server (12), predicting that they may be *O*-glycosylated (Fig. 1*B*).

Next, we utilized the isoform-specific *O*-glycosylation Predictor (ISOGlyP: http://isoglyp.utep.edu)[4] for comparison (Fig. 1*B*) and found that two of these sites were most likely *O*-glycosylated: Thr^{23} (by GalNAc T-1, -2, and -11–13) and Thr^{36} (by GalNAc T-1–3, -5, -11–14, and 16), each having enhancement value products (EVP) values greater than 1.0 as shown in Fig. 1*B* and Table S1 (9, 13, 14). However, it is unlikely that Thr^{36} is *O*-glycosylated as *N*-glycosylated Asn^{34} would be expected to act as an obstruction and because Thr^{36} is part of the *N*-glycosylation motif (N*X*T) that is strictly conserved in vertebrate OPSR/OPSG. In this work, we took advantage of a monoclonal antibody (7G8 mAB) raised in-house against hOPSG expressed

[4] Please note that the JBC is not responsible for the long-term archiving and maintenance of this site or any other third party hosted site.

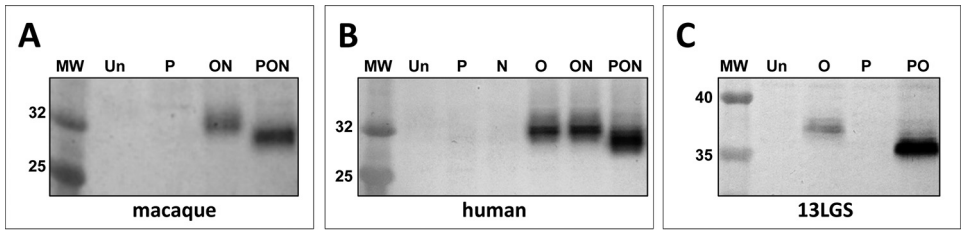

Figure 2. *O*-Glycosylation of red/green cone opsins in retina of Euarchontoglires. 7G8 mAB immunoblots of retinal detergent extracts treated with different glycosidases. The retina tissues were obtained from macaque (*A*), human (*B*) and 13LGS eyes (*C*). The *lanes labeled with letters* correspond to the enzymatic treatment of the samples: untreated (*Un*), treated with *O*-glycosidase (*O*), PNGase F (*P*), and/or neuraminidase (*N*).

in Sf9 cells, whose epitope (^{21}DSTQSSIF^{28}) contains Thr^{23} and two Ser residues predicted to be *O*-glycosylated by NetOGlyc 4.0. The epitope of 7G8 mAB was first refined by immunoblotting with several deletion variants of hOPSG expressed in Sf9 cells (Fig. S1*A*). Subsequently, the precise determination of the 7G8 mAB epitope was achieved by using immunoblots of a hOPSG construct expressed in Sf9 cells and incubating the membrane with 7G8 mAB in the presence of overlapping competing peptides (Fig. S1, *B* and *C*).

We theorized that if any of the Ser or Thr residues in the 7G8 mAB epitope were *O*-glycosylated, 7G8 mAB would be unable to bind OPSR/OPSG. We first tested this hypothesis with human and monkey retinal extracts, and then with other species to assess the prevalence of *O*-glycosylation of OPSR/OPSG in mammals, which would indicate the biological significance of this PTM in photoreceptor function or structure.

Macaques

Although 7G8 mAB was raised against hOPSG expressed in Sf9 cells, the antibody was unable to recognize macaque OPSR/OPSG in immunoblots of retinal extracts (Fig. 2*A*, *lane Un*). Furthermore, the removal of *N*-glycans with PNGase F had no effect on the binding of 7G8 mAB (Fig. 2*A*, *lane P*). However, treatment of the macaque retinal extract with *O*-glycosidase plus neuraminidase resulted in the binding of 7G8 mAB to macaque OPSR/OPSG (Fig. 2*A*, *lanes ON* and *PON*). These two enzymes are typically used in combination for the removal of terminal sialic acid residues (by neuraminidase) and core 1 disaccharide *O*-glycans (by *O*-glycosidase), demonstrating that macaque OPSR/OPSG is *O*-glycosylated by relatively short glycans on the epitope of 7G8 mAB.

Humans

Next, we explored whether 7G8 mAB could bind to OPSR/OPSG from human retinal extracts. 7G8 mAB was able to bind hOPSR/hOPSG deglycosylated with *O*-glycosidase treatment alone (Fig. 2*B*, *lane O*), demonstrating that hOPSR/hOPSG is also *O*-glycosylated and that the *O*-glycans (at least those corresponding to the epitope of 7G8 mAB) are not highly capped by sialic acid. As expected, further treatment of hOPSR/OPSG with PNGase F resulted in a band shift of ~2 kDa (Fig. 2*B*, *lane PON*).

Thirteen-lined ground squirrels

13LGS are extensively used for color vision research because they have cone-dominant retinas (15). Because the epitope for 7G8 mAB is conserved in OPSG of 13LGS, we used this antibody to demonstrate that the OPSG of these rodents is also *O*-glycosylated. Like humans, *O*-glycans at the epitope of 7G8 mAB could be removed with *O*-glycosidase treatment alone (Fig. 2*C*, *lanes O* and *PO*).

The marked difference in band intensity between *lanes O* and *PO* in Fig. 2*C* is most likely due to the proximity of Asn^{34} to the epitope of 7G8 mAB. The presence of *N*-glycans on Asn^{34} results in weaker 7G8 mAB-binding affinity to OPSG due to steric hindrance. To reduce this artifactual difference in band intensity (between *lanes O* and *PO*), the polyvinylidene fluoride (PVDF) membrane was incubated with PNGase F after protein transfer, thus removing most of the *N*-glycans that lessened the binding of 7G8 mAB to OPSG (Fig. S2).

Pigs

We then investigated whether *O*-glycosylation at the N terminus of OPSR/OSPG is a general PTM among mammals. The epitope of 7G8 mAB is present in OPSR/OSPG of most Euarchonta (proposed grandorder of mammals that includes primates) and squirrels. However, the porcine OPSG sequence contains a change in one residue with respect to the epitope of 7G8 mAB (Ser^{25} → Gly^{25}), which results in weaker antibody affinity. We tested porcine retinal extracts with 7G8 mAB, and OPSG bands were visible in immunoblots only for those samples treated with *O*-glycosidase (Fig. S3*D*), demonstrating that porcine OPSG is also *O*-glycosylated at the N terminus.

Cows

Like porcine OPSG, the sequence of bovine OPSR contains two residue changes with respect to the epitope of 7G8 mAB (Asp^{21} → Glu^{21} and Ser^{25} → Gly^{25}). ROS prepared from bovine retinas by sucrose density gradient centrifugation (16) contain a small amount of cone outer segments (COS). However, 7G8 mAB did not detect the bOPSR band in immunoblots of bovine COS/ROS detergent extracts treated with *O*-glycosidase, apparently due to weak binding affinity and high background. However, when bOPSR was semi-purified by cation-exchange chromatography from COS/ROS detergent extracts, the 7G8 mAB was able to detect bOPSR upon treatment with *O*-glycosidase (Fig. S3*G*). These results suggest that *O*-glycosylation of OPSR/OPSG is a PTM likely present in all mammals.

Molecular weight shifts of OPSR/OPSG upon removal of O-glycans

Once established that the N terminus of hOPSR/hOPSG is *O*-glycosylated, we estimated the total amount of *O*-glycans per opsin molecule. To reduce background and nonspecific anti-

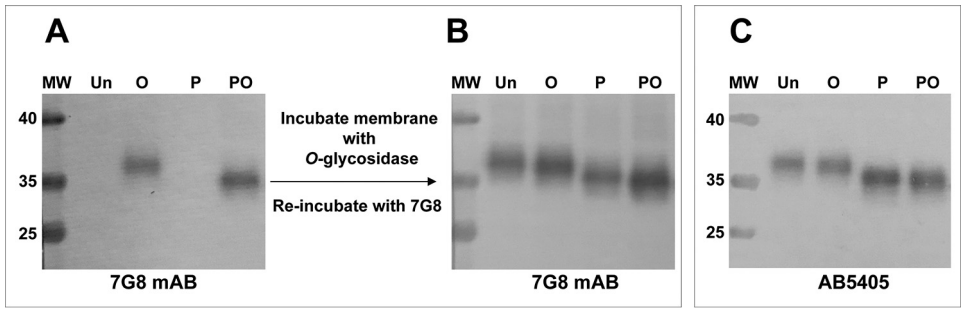

Figure 3. *O*-Deglycosylation of human red/green cone opsins on PVDF membrane. hOPSR/hOPSG from a human retinal detergent extract was immunoprecipitated with nanobody Nb-E9. The sample was treated with different glycosidases, subjected to SDS-PAGE, and transferred simultaneously to two PVDF membranes. *A,* top immunoblot of *red/green* cone opsins incubated with 7G8 mAB. The *lanes labeled with letters* correspond to the enzymatic treatment of the samples: untreated (*Un*), treated with *O*-glycosidase (*O*), and/or PNGase F (*P*). *B,* membrane from *A* was washed, incubated with *O*-glycosidase, re-incubated with 7G8 mAB, and developed again. *C,* immunoblot of bottom membrane incubated with anti-C terminus polyclonal antibody AB5405.

body binding, we used immunoprecipitated hOPSR/hOPSG instead of retinal detergent extracts. The samples, incubated with different glycosidases, were subjected to SDS-PAGE and transferred simultaneously to two PVDF membranes. The top membrane was incubated with 7G8 mAB, and as expected, it detected bands only for those samples treated with *O*-glycosidase (Fig. 3*A*, *lanes O* and *PO*). The developed membrane was then treated with *O*-glycosidase, re-incubated with 7G8 mAB and re-developed. Applying this strategy, the bands of *O*-glycosylated OPSR/OPSG, previously undetected by 7G8 mAB, were now visible (Fig. 3*B*, *lanes Un* and *P*). These results demonstrate that the *O*-glycosylation of hOPSR/hOPSG is composed of short, relatively homogeneous glycans and that the molecular mass shift upon *O*-deglycosylation is small, ~0.5 kDa (Fig. 3*B*).

To further confirm that the bands observed in 7G8 mAB immunoblots correspond to hOPSR/hOPSG, the bottom PVDF membrane was incubated with the anti-red/green opsin antibody AB5405. This is a rabbit polyclonal antibody raised against the C terminus of hOPSR/hOPSG (17). Fig. 3*C* shows that the bands detected by anti-C-terminal AB5405 antibody are the same as the bands detected by the anti-N-terminal 7G8 mAB in Fig. 3*B*.

The same experimental strategy was then used for samples from other mammalian species, confirming a small M_r shift upon *O*-deglycosylation of OPSR/OPSG from 13LGS (Fig. S3*B*), pigs (Fig. S3*E*), and cows (Fig. S3*H*). Additionally, retinal samples of 13LGS (Fig. S3*C*) and pigs (Fig. S3*F*) were subjected to immunoblotting with antibody AB5405, confirming the identity of the bands observed in 7G8 mAB immunoblots.

In the case of bOPSR, the situation appears to be more complex than for the other mammalian species investigated. Comparison of immunoblots of bOPSR incubated with anti-N-terminal 7G8 mAB and with anti-C-terminal AB5405 antibody reveals the existence of additional, less homogeneous bOPSR species of higher M_r for the immunoblot incubated with AB5405 antibody (Fig. S3*I*). These new species, undetected by 7G8 mAB but revealed by AB5405 antibody, suggest the presence of more complex and longer *O*-glycans at the N terminus that are refractory to *O*-glycosidase treatment, which only cleaves short core 1 *O*-glycans. The estimated molecular mass shift following *O*-deglycosylation of OPSR/OPSG for different mammals (0.4 – 0.7 kDa) (see Figs. 3*B* and Fig. S3) indicates the presence of two or three monosaccharides modifying each OPSR/OPSG molecule.

Because of sequence divergence (see Fig. 1*A*), 7G8 mAB is not expected to recognize *O*-deglycosylated OPSR/OPSG from other mammalian and vertebrate species. However, immunoblots incubated with anti-C-terminal antibody AB5405 can reveal small electrophoretic shifts upon removal of *O*-glycans from OPSR/OPSG of species not typically recognized by 7G8 mAB, as shown for mouse OPSG in Fig. S4. Similar mobility shifts upon removal of *O*-glycans can be observed for OPSR/OPSG of 13LGS, pig, and cow in immunoblots incubated with antibody AB5405 (Fig. S3, *C, F,* and *I*).

Binding of jacalin to OPSR and OPSG

Jacalin is a lectin from the seeds of jackfruit (*Artocarpus integrifolia*) that binds *O*-glycans. Although its specificity for galactosyl (β-1,3) GalNAc (T-antigen) is overstated, functional studies show that jacalin has a strong binding preference toward GalNAcα1 peptides, in which the C6-OH of αGalNAc is free (18). In our studies, jacalin recognized *N*-deglycosylated hOPSR/hOPSG in lectin blots (Fig. 4*A*), which further supports the presence of *O*-glycans on these human cone opsins. The electrophoretic mobility of the bands detected by jacalin was identical to the bands detected by AB5405 antibody (Fig. 4*B*), which confirms the identity of hOPSR/hOPSG. As expected, 7G8 mAB only detected the samples in which the *O*-glycans had been removed by *O*-glycosidase (Fig. 4*C*).

In a similar manner, we also confirmed in lectin blots incubated with jacalin the presence of *O*-glycans in OPSR/OPSG from retinas of chicken (Fig. 4*D*), *Xenopus* (Fig. 4*E*), 13LGS (Fig. 4*F*), and pig (Fig. 4*G*). The identity of the bands detected by jacalin was confirmed with immunoblots using antibody AB5405.

Identification of glycosylation sites by mass spectrometry

To determine the *O*-glycosylation site(s) of mammalian OPSR/OPSG and the composition of its glycan(s), we resorted to MS analyses of bovine OPSR purified from cow retinas.

bOPSR was purified from bovine retina using sucrose density gradient centrifugation, cation-exchange chromatography (Fig. 5), and precipitation with immobilized jacalin (Fig. S5). Purified proteins were then treated with PNGase F for removal of

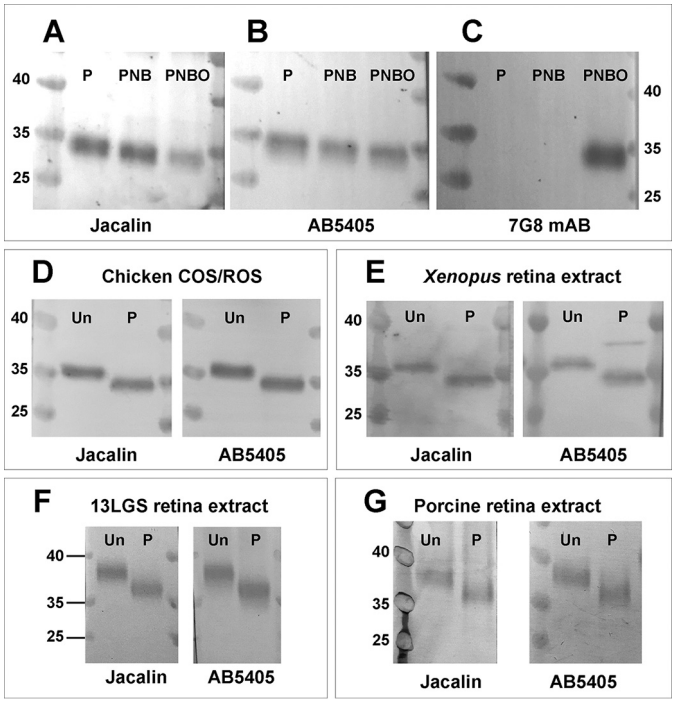

Figure 4. Jacalin binds to OPSR/OPSG of different vertebrates in immunoblots. *A–C,* hOPSR/hOPSG purified from human retina was treated with different glycosidases, subjected to SDS-PAGE, and transferred simultaneously to three PVDF membranes. *A,* top membrane, incubated with jacalin; *B,* middle membrane, incubated with anti-C-terminal antibody AB5405; *C,* bottom membrane, incubated with 7G8 mAB. *D–G,* Jacalin blots and AB5405 immunoblots of chicken COS/ROS samples (*D*), and of retinal extracts from *X. laevis* (*E*), 13LGS (*F*), and pig (*G*). The *lanes labeled with letters* correspond to the enzymatic treatment of the samples: untreated (*Un*), treated with PNGase F (*P*), neuraminidase (*N*), β(1–3)-galactosidase (*B*) and/or *O*-glycosidase (*O*).

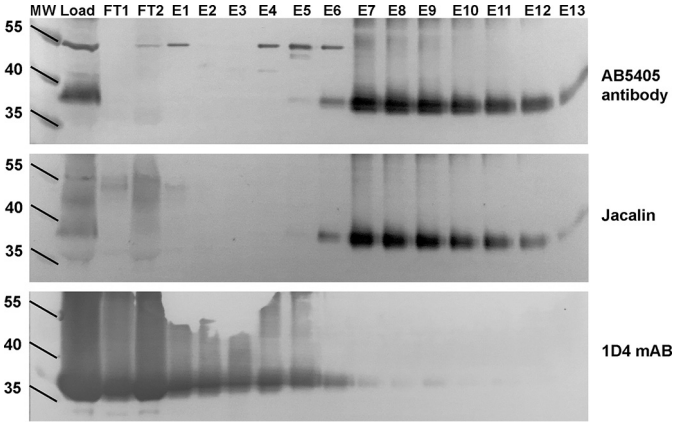

Figure 5. Purification of bOPSR by cation-exchange chromatography. An LMNG-solubilized bovine COS/ROS sample was loaded onto a column equilibrated with 10 mM HEPES, pH 7. 4, 10 mM NaCl, 0.2 mM LMNG, and it was eluted with a NaCl gradient (0.01–2 M) in 12 fractions, followed by further elution at 2 M NaCl. The samples and fractions were subjected to SDS-PAGE; the proteins in the gel were transferred simultaneously to three PVDF membranes, and the membranes were incubated for blot analysis with anti-hOPSR/hOPSG polyclonal antibody AB5405, jacalin, or anti-rhodopsin 1D4 mAB. *FT,* flow-through; *En,* elution fraction *n*.

N-linked glycosaccharides and separated via SDS-PAGE (see under "Experimental procedures"). Protein bands corresponding to bOPSR were excised and digested with trypsin. The resulting peptides were analyzed by LC MS/MS to identify the *O*-glycosylation site and composition, as well as confirm the *N*-glycosylation site.

Protein database searching of MS data unambiguously identified Ser^{22} as the *O*-glycosylated residue and Asn^{34} as the *N*-glycosylation site (Fig. 6). MS/MS analysis of a parent ion (m/z 1124.5060^{3+}) yielded a series of b and y ions accurately identifying the peptide as ^{10}LAGGQPQANFEESTQGSIFTYTNSNSTR^{37}, in which the 13th residue (Ser^{22}) was modified with a Hex-HexNAc *O*-glycan and the 25th residue (Asn^{34}) was deamidated, representing an *O*-glycosylated peptide with *N*-glycan removed by PNGase F cleavage (Fig. 6 and Table S2). In addition, the same m/z ion was repetitively sequenced, and potentially represents another *O*-glycosylated peptide with the same sequence as described above. However, due to lack of specific fragment ions, the actual site cannot be unambiguously determined. In addition to Ser^{22}, we suspect that Thr^{23} and/or Ser^{26} may represent additional *O*-glycosylation sites in bOPSR.

The only unambiguously *O*-glycan detected on Ser^{22} is consistent with Gal–GalNAc-, as bOPSR was purified with immobilized jacalin. However, this species seems to form the majority of the bOPSR band identified by the antibody AB5405 (see Fig. 5 and Fig. S5). Several other minor glycopeptide species (with Hex–HexNAc and Hex–$HexNAc_2$ as major *O*-glycans) were identified but had ambiguous *O*-glycosylation sites due to the proximity of Ser and Thr residues.

The observed deamidation of Asn^{34} in PNGase F-treated bOPSR confirms it as the *N*-glycosylated residue in mammalian OPSR/OPSG in native tissues, as expected, as it is part of the *N*-glycosylation motif N*X*(S/T) (where *X* is any amino acid, except Pro).

Regeneration of N-terminal deletion variants of hOPSG with 11-cis-retinal

The N-terminal domain of rhodopsin forms a plug for the chromophore-binding pocket (19, 20), and it is expected that the N terminus of cone opsins has the same function (21). Because the N terminus of hOPSR/hOPSG is more than 16 residues longer than the N termini of rhodopsin and blue cone opsin (Fig. 1*A*), we speculated that *O*-glycosylation might have a protective role against proteolysis and that its cleavage C-terminal to the epitope of 7G8 mAB might compromise the function of the protein. For this reason, the functionality of a full-length hOPSG construct was compared with that of three deletion variants (Δ16N, Δ27N, and Δ43N OPSG/T4L, Fig. 7*A*) expressed in Sf9 cells. All four constructs had the insertion of T4L into the intracellular loop 3, which does not affect hOPSG regeneration with 11-*cis*-retinal (22, 23). The constructs were regenerated with 11-*cis*-retinal, purified at similar concentrations (as estimated by SDS-PAGE and Coomassie-staining) (Fig. 7*B*), and their absorption spectra compared.

In agreement with previous studies (23), the deletion of the 16 N-terminal residues of OPSG/T4L did not adversely affect its regeneration with 11-*cis*-retinal ($A_{530\ nm}$, Fig. 7*C*). However, an OPSG deletion variant missing its 27 N-terminal residues (Δ27N OPSG/T4L) had significantly lower regeneration efficiency when compared with the OPSG/T4L and Δ16N OPSG/T4L constructs. Finally, a construct missing the 43 N-terminal residues (Δ43N OPSG/T4L) was unable to bind 11-*cis*-retinal (Fig. 7*C*). These data indicate that the integrity of the C-terminal half of hOPSG's N terminus is essential for its function,

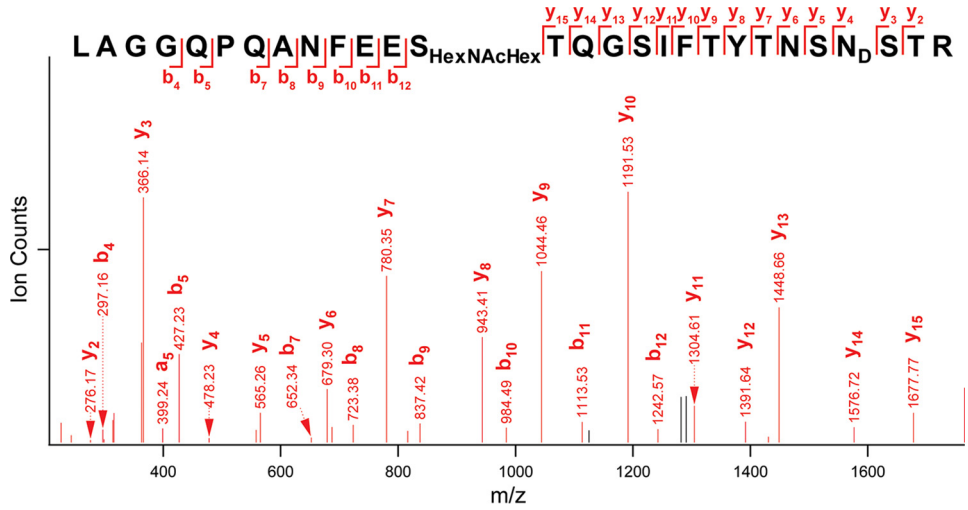

Figure 6. Identification of *O*-glycosylated peptide by MS/MS analysis. Fragmentation of a precursor ion (*m/z* 1124. 5060^{3+}) using high-energy collisional dissociation during MS/MS analysis yielded a series of b and y ions that accurately identified the peptide as ^{10}LAGGQPQANFEESTQGSIFTYTNSNSTR^{37}, in which the 13th residue (Ser^{22}) was *O*-glycosylated and the 25th residue (Asn^{34}) was deamidated. Matched ions are shown in *red*; internal fragmentation ions are not labeled in the spectrum.

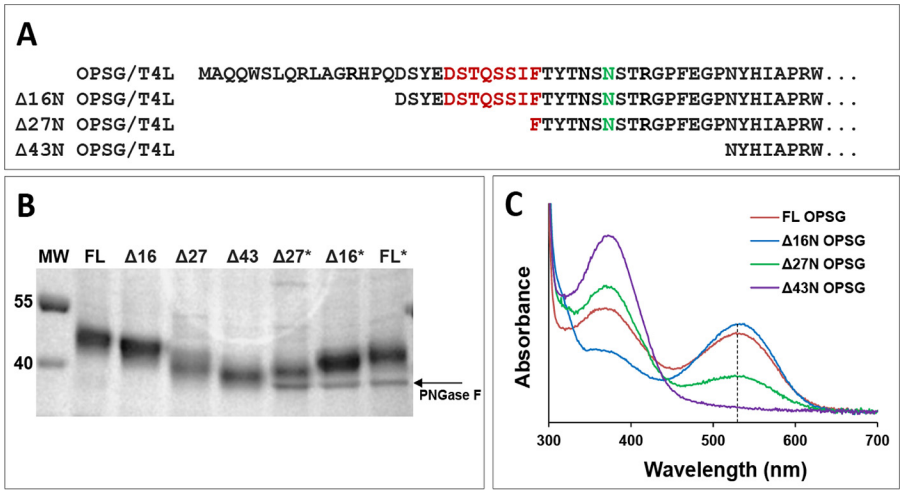

Figure 7. Regeneration with 11-*cis*-retinal of hOPSG deletion constructs expressed in Sf9 cells. In all constructs, intracellular loop 3 was replaced by T4L, and the 1D4 mAB epitope was fused at the C terminus. *A,* N-terminal sequence of the four constructs used in this figure. *B,* Coomassie-stained SDS-PAGE of the four immunopurified OPSG/T4L constructs: full-length OPSG/T4L (*FL*), Δ16N OPSG/T4L (*Δ16*), Δ27N OPSG/T4L (*Δ27*), and Δ43N OPSG/T4L (*Δ43*). The relative band intensities (normalized to that of Δ16N) were 0.94, 1, 0.62, and 0.66 for FL, Δ16N, Δ27N, and Δ43N OPSG/T4L, respectively. The three samples labeled with an *asterisk* had been incubated with PNGase F. *C,* absorbance spectra of the four purified OPSG/T4L constructs. The absorbance was normalized to account for the molecular mass of the constructs and their respective electrophoretic band intensity in *B*. The discontinuous line marks the $A_{530\ nm}$.

suggesting that *O*-glycosylation might have a protective role against proteolysis.

O-Glycosylation of hOPSR/hOPSG expressed in heterologous systems

Because research on cone opsins is often done using recombinant proteins, we decided to investigate whether hOPSG expressed in insect and mammalian cells is *O*-glycosylated in a manner similar to native tissues.

Mammalian HEK293 and HEK293SGnTI$^-$ cells

Immunoblots of hOPSG expressed in *N*-glycosylation–deficient HEK293SGnTI$^-$ cells (6) and stained with 7G8 mAB suggest a homogeneous *N*-glycosylation pattern (Fig. 8*A*), where one main band is observed in both lanes, with a minor population of non-*N*-glycosylated hOPSG. However, when the same samples were subjected to immunoblotting with the anti-C-terminal 1D4 mAB (Fig. 8*B*), an extra band of similar intensity but reduced electrophoretic mobility is evident (Fig. 8*B*,

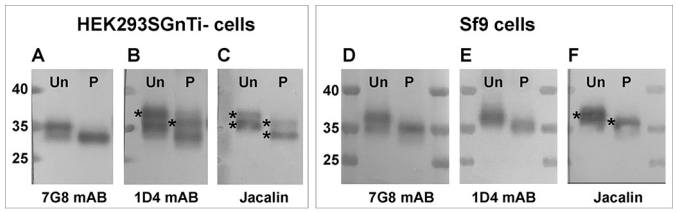

Figure 8. Human green cone opsin expressed in mammalian and insect cells is partially *N*- and *O*-glycosylated. *A–C,* immunoblots of purified hOPSG expressed in *N*-glycosylation–deficient HEK293SGnTI$^-$ cells, incubated with anti-N terminus 7G8 mAB (*A*), anti-C terminus 1D4 mAB (*B*), or jacalin (*C*). *D–F,* immunoblots of purified hOPSG expressed in *Sf9* cells, incubated with anti-N terminus 7G8 mAB (*D*), anti-C terminus 1D4 mAB (*E*), or jacalin (*F*). The bands marked with an *asterisk* are not detected by 7G8 mAB. The samples were untreated (*Un*) or treated with PNGase F (*P*).

bands marked with an *asterisk*). Treatment with *O*-glycosidase alone did not cause a noticeable mobility shift, but neuraminidase treatment resulted in an increased mobility of the top band, but insufficient to merge with the lower band (Fig. S6*A*). The presence of a band on 1D4 mAB immunoblots that is undetectable by 7G8 mAB indicates the presence of PTMs (probably sialylated *O*-glycans) on or near the 7G8 mAB epitope.

Like 1D4 mAB, jacalin recognized two electrophoretic bands, although the intensity of the top band was weaker than that of the bottom band, and the bottom band had an apparent molecular mass ~0.7 kDa larger than the band detected by 7G8 mAB (Fig. 8*C*). These results indicate that hOPSG expressed in HEK293SGnTI$^-$ cells consists of a mixture of at least four separate species: a nonglycosylated and an *N*-glycosylated only species (both detected by 7G8 and 1D4 mABs), an *N*- and *O*-glycosylated species with small *O*-glycans (revealed mainly by jacalin and more weakly by 1D4 mAB), and another species carrying both *N*-glycans and sialylated complex *O*-glycans (detected by 1D4 mAB and more weakly by jacalin).

A more complex case is observed for hOPSG expressed in HEK293 cells (Fig. S6, *B* and *C*). Although the anti-N-terminal 7G8 mAB immunoblots show two bands that merge into one band upon treatment with PNGase F (Fig. S6*B*) (suggesting incomplete *N*-glycosylation), the anti-C-terminal 1D4 mAB immunoblots reveal a highly heterogeneous, high-molecular weight pattern suggesting extensive *N*- and *O*-glycosylation, with most of these species being undetectable with 7G8 mAB (Fig. S6*C*). The lack of 7G8 mAB detection is likely due to the presence of *O*-glycans and, to a lesser extent, the presence of large *N*-glycans at Asn^{34}, which would prevent 7G8 binding due to steric hindrance.

Insect Sf9 cells

Insect cells are able to modify proteins with *O*-glycans (24). Jacalin blots of Sf9-expressed hOPSG showed bands with an apparent molecular mass ~0.8 kDa larger than the bands revealed by anti-N-terminal 7G8 mAB (and ~0.7 kDa larger the bands revealed by anti-C-terminal 1D4 mAB) (Fig. 8). In other words, the center mass of the bands revealed by 1D4 have an electrophoretic mobility much closer to the 7G8 bands than to the jacalin bands (see Fig. 8), which suggests that the majority of OPSG species does not carry *O*-glycans.

Discussion

In this study, we demonstrated that the vertebrate cone visual pigments OPSR and OPSG are *O*-glycosylated at an N-terminal Ser/Thr-rich sequence that forms part of the 7G8 mAB epitope, with a full occupancy and in a relatively homogeneous manner. Supporting evidence for this finding included the inability of 7G8 mAB to bind OPSR/OPSG from the retina of different mammals (including humans) unless their *O*-glycans had been removed enzymatically. MS analysis then identified residue Ser^{22} as the *O*-glycosylation site in bovine OPSR. Lectin blots incubated with jacalin and sequence conservation of Ser^{22} suggest that *O*-glycosylation likely is present in OPSR/OPSG of all vertebrates. Although Ser^{22} seems to be the preferred *O*-glycosylated residue of bOPSR, the precise *O*-glycosylation site might not be critical, as there is Ser/Thr redundancy in the N-terminal domain and sequence variability among species (see Fig. 1*A*). This evolutionary conservation implies that *O*-glycosylation of OPSR/OPSG likely has a role in determining photoreceptor structure/function.

A variety of GPCRs has been found to be *O*-glycosylated at their N termini, and the role proposed for this PTM depends on the specific GPCR. For example, it has been proposed that *O*-glycosylation in the β1-adrenergic receptor regulates N-terminal cleavage (25), whereas for the δ-opioid receptor it modulates turnover at the plasma membrane (26). In addition to the β1-adrenergic receptor, other GPCRs from different subfamilies have been reported to undergo N-terminal cleavage mediated by metalloproteinases. Interestingly, almost all the GPCRs reported to undergo N-terminal cleavage have been identified (or are predicted) to be *O*-glycosylated in proximity to the reported cleavage sites. Therefore, proximal (or adjacent) site-specific *O*-glycosylation could reduce, enhance, or displace proteolytic cleavage sites, as well as direct the proteases involved (11).

The role of *O*-glycosylation at the N termini of vertebrate OPSR and OPSG is unclear. Comparison of the amino acid sequences of the human visual opsins shows that OPSR and OPSG have longer N termini than rhodopsin and blue cone opsin. Whereas the integrity of rhodopsin's N terminus is required for the efficient regeneration with 11-*cis*-retinal (27), OPSR and OPSG can tolerate deletions of at least 16 N-terminal residues without affecting their ability to bind chromophore. In addition to *N*-glycosylation at Asn^2 and Asn^{15}, rhodopsin is protected against N-terminal proteolysis by the acetylation of Met^1. We can speculate that *O*-glycosylation of the OPSR and OPSG N termini might prevent proteolytic cleavage as well, because the deletion of the *O*-glycosylated Ser/Thr-rich segment (part of epitope of 7G8 mAB) compromises its regeneration with 11-*cis*-retinal. Another possible function of *O*-glycosylation in OPSR and OPSG might be related to opsin transport and/or cone cell disc formation, perhaps with the participation of galectins. Galectins typically bind β-galactose-containing glycoconjugates and have diverse biological functions, including roles in development, regulation of immune cell activities, and microbial recognition as part of the innate immune system (28). For example, Drgal1–L2 is a galectin secreted by retinal stem cells and photoreceptor progenitors that is required for the regeneration of injured rod photoreceptors in zebrafish (29). Thus, the presence of short *O*-glycosidase–sensitive *O*-glycans terminating in β-galactose is consistent with the potential for galectin–OPSR/OPSG interactions.

As for visual opsins, *O*-glycosylation has been reported to modify octopus rhodopsin (an invertebrate opsin more closely related to melanopsin than to vertebrate rhodopsin) (30). Sugar composition analysis performed in the same work suggested that chicken OPSR (iodopsin) is also *O*-glycosylated, with 2.8 GalNAc residues per opsin molecule, which is in good agreement with this work.

Whereas most *O*-glycans of OPSR and OPSG extracted from mammalian retinas do not appear to be highly capped by sialic acid, the same cone opsins expressed in HEK293SGnTI$^-$ cells

(and likely HEK293 cells) are expressed as a mixture of non-*O*-glycosylated, *O*-glycosylated, and sialylated species. In the case of OPSG expressed in insect Sf9 cells, the *O*-glycan occupancy seems very limited. This work highlights the fact that heterologous expression systems often fail to recapitulate the PTMs of native proteins.

Bovine OPSR seems to have an *O*-glycosylation pattern more heterogeneous than OPSR/OSPG from other species investigated, although the glycopeptides identified by MS correspond to the subset purified by immobilized jacalin. Also, note that the sequence of bOPSR is not identical to that of hOPSR/hOPSG (see Fig. 1*C*), resulting in slightly different *O*-glycosylation prediction scores for Ser^{22} (*i.e.* maximum ISOGlyP EVP value of Ser^{22} is 0.18 for bOPSR *versus* 0.34 for hOPSR/hOPSG, and NetOGlyc 4.0 gives a score of 0.55 for bOPSR *versus* 0.42/0.50 for hOPSR/hOPSG). These results highlight the difficulty of predicting *O*-glycosylation sites on proteins, although both algorithms were able to predict the existence of an *O*-glycosylation domain. Future studies are needed to determine the role of *O*-glycosylation in cone opsin function and/or cone cell development. This last goal can be achieved by studying the effects of point mutations preventing *O*-glycosylation in OPSR and OPSG expressed in model organisms.

Experimental procedures

Retinal detergent extracts

All experiments were approved by the Institutional Animal Care and Use Committees at Case Western Reserve University (IACUC protocol no. 2014-0071) and University of California, Irvine (IACUC protocol no. AUP18-124), and were conducted in accordance with the Association for Research in Vision and Ophthalmology Statement for the Use of Animals in Ophthalmic and Visual Research.

Human retinas were generously donated by Dr. Irina Pikuleva (Case Western Reserve University, Cleveland, OH). Macaque (*Macaca fascicularis*) retinas were a gift from Dr. Grazyna Palczewska (Polgenix, Inc., Cleveland, OH) after being subjected to retinoid extraction in hexane. 13LGS (*Ictidomys tridecemlineatus*) eyes were generously donated by Dr. Joseph Carroll and Ben Sajdak (Medical College of Wisconsin, Milwaukee, WI). Porcine (*Sus scrofa*) eyes were donated by J. H. Routh Packing Co. (Sandusky, OH). *Xenopus laevis* retinas were obtained from Dr. Yoshikazu Imanishi (Case Western Reserve University, Cleveland, OH). Chicken (*Gallus gallus*) heads were obtained from a local butcher shop. Bovine (*Bos taurus*) eyes were obtained from local slaughterhouses. Retinas were removed from eyeballs with tweezers and frozen at −80 °C until further use. Retinal detergent extracts were prepared as follows: retinas were sonicated in 40 mM phosphate buffer, pH 7.4, containing 10.8 mM KCl, 548 mM NaCl (plus protease inhibitors, 1 mM $MgCl_2$ and DNase). An equal volume of 1% lauryl maltose neopentyl glycol (LMNG) was added, the mixture was sonicated briefly and rotated 1 h at 4 °C, and the samples were centrifuged for 10 min at 21,000 × *g*. Finally, the supernatant was filtered through a 0.22-μm filter.

Purification of OPSR and OPSG from detergent extracts

In the case of murine and bovine retinal detergent extracts, immunoblots suffered from high background due to nonspecific binding of antibody, low cone opsin content, and/or low antibody affinity. To increase the quality of 7G8 mAB immunoblots, bOPSR was semi-purified by cation-exchange chromatography (described below). To improve the quality of 7G8 mAB immunoblots for molecular weight shift determinations, hOPSR/hOPSG and murine OPSG were enriched by immunoprecipitation (described below).

To purify bOPSR for MS studies, COS/ROS were isolated from bovine retinas following a protocol described previously (16). The membranes were then solubilized in 10 mM HEPES, pH 7.4, 10 mM NaCl, 5 mM LMNG and loaded onto a cation-exchange column (Macro-Prep High S, Bio-Rad) in normal light conditions. The column was eluted with a linear gradient from 10 mM to 2 M NaCl, and bOPSR was eluted at 1–1.5 M NaCl (see Fig. 5). Most rhodopsin and other proteins eluted at lower NaCl concentrations. The fractions containing bOPSR (but still with rhodopsin as the major component) were combined and dialyzed against 10 mM HEPES, pH 7.4, 150 mM NaCl, 0.2 mM LMNG. For further purification, bOPSR was captured by agarose-immobilized jacalin (Vector Laboratories, Burlingame, CA), washed, and eluted with 0.2 M melibiose in 10 mM HEPES, pH 7.4, 150 mM NaCl, 0.2 mM LMNG. Next, proteins were *N*-deglycosylated with PNGase F, separated by SDS-PAGE, and detected with silver (Fig. S5) or Coomassie staining. The band corresponding to bOPSR was excised from the gel and de-stained, and bOPSR was digested with trypsin for MS analysis.

Mouse OPSG and human hOPSR/hOPSG were immunoprecipitated using a llama antibody (Nb-E9 nanobody) raised against hOPSG purified from *Sf9* cells.[5] Briefly, LMNG-solubilized retinal extracts were incubated with His-tagged Nb-E9 bound to TALON immobilized metal affinity resin (Clontech). Subsequently, the TALON resin was washed with 40 mM phosphate buffer, pH 7.4, containing 10.8 mM KCl, 548 mM NaCl, 0.25 mM LMNG, 10 mM imidazole and finally the complex of Nb-E9 with OPSR/OPSG was eluted with 0.2 M competing imidazole. Chicken COS/ROS were prepared by adapting the method for ROS isolation from bovine retinas (16).

Lectin blotting and immunoblotting

Typically, retinal detergent extracts (or purified protein) were incubated with 1/100 volumes of 0–4 types of glycosidases for 6 h on ice. His-tagged PNGase F was prepared in-house and purified by immobilized metal affinity chromatography to 1 mg/ml. *O*-Glycosidase (endo-α-*N*-acetylgalactosaminidase, 40,000,000 units/ml), β1–3 galactosidase (10,000,000 units/ml), and α2–3,6,8 neuraminidase (50,000,000 units/ml) were purchased from New England Biolabs (Beverly, MA).

Samples were loaded on NuPAGE™ 4–12% BisTris protein gels (Thermo Fisher Scientific, Carlsbad, CA) and subjected to electrophoresis with MOPS buffer. Proteins on the gel were

[5] D. Salom, H. Jin, and K. Palczewski, manuscript in preparation.

transferred simultaneously to 1–3 PVDF membranes. The membranes were blocked with 25 mM Tris, pH 7.4, 140 mM NaCl, 3 mM KCl, 0.1% Triton X-100 (TBST) containing 5% fat-free milk (for immunoblots) or 2–4% polyvinylpyrrolidone 40 (for lectin blots). After incubation with the appropriate antibody or lectin, the membranes were washed three times with TBST and developed with the alkaline phosphatase (AP) reaction (color development substrates are 5-bromo-4-chloro-3-indolyl-phosphate and nitro blue tetrazolium, Promega, Madison, WI). Before use, jacalin (Vector Laboratories, Burlingame, CA), 7G8 mAB, and 1D4 mAB were coupled to AP using a Lightning-Link labeling kit from Innova Biosciences (Babraham, Cambridge, UK). An AP-conjugated anti-rabbit secondary antibody (Promega, Madison, WI) was used for immunoblots with antibody AB5405.

Commercial polyclonal antibody AB5405 (Millipore, Billerica, MA; lot no. 2880810) was raised in rabbit against a His-tagged peptide corresponding to the C terminus of hOPSR/hOPSG. This antibody cross-reacts with His-tagged PNGase F used in some experiments (for example, see Fig. 4*E* and Fig. S3, *C, F,* and *I*). However, when the proteins were transferred from the gel simultaneously to two or more PVDF membranes, the band corresponding to PNGase F was absent from the bottom membranes (see as example Fig. 3*C*). In a similar manner, for lectin blots, background was reduced in the bottom membranes.

To estimate the molecular weight shift of OPSR/OPSR upon *O*-deglycosylation (Fig. 3 and Fig. S3), PVDF membranes previously incubated with AP-coupled 7G8 mAB and developed were incubated overnight with 40,000 units of *O*-glycosidase in 10 mM HEPES, pH 7.0, 0.1 M NaCl, 0.2 mM LMNG at 4 °C. The membrane then was re-incubated with 7G8 mAB and developed again.

Generation of mABs against hOPSG

7G8 mAB was raised against 1D4-immunopurified hOPSG expressed in Sf9 cells (22) by immunizing mice following standard methods (31). Briefly, 30–50 μg of purified hOPSG was emulsified with adjuvant (Sigma) before intraperitoneal (i.p.) injection into a 4–5-week-old female BALB/c mouse (The Jackson Laboratory, Bar Harbor, ME). The injection was repeated 3–4 times in 10-day intervals or until the serum titer increased 100–1000-fold. The immunized mouse was then sacrificed, and the spleen was fused with Sp2/0-Ag14 myeloma cells (ATCC, Manassas, VA; CRL-1581). Stable hybridoma cell lines were generated using a ClonaCell-HY Hybridoma kit (Stemcell Technologies, Vancouver, Canada) by the Case Visual Sciences Research Center Grant EY11373. 7G8 mAB secreted into the hybridoma medium was purified at 1 mg/ml with a 1-ml HiTrap protein A HP antibody purification column (GE Healthcare). The determination of the 7G8 mAB epitope is detailed in Fig. S1.

Liquid chromatography tandem MS (LC MS/MS)

Purified bOPSR was treated with PNGase F, separated using SDS-PAGE, and visualized using Coomassie Blue. Bands corresponding to bOPSR were excised, reduced with tris(2-carboxyethyl)phosphine for 30 min, and alkylated with chloroacetamide in the dark for 30 min at room temperature. Following tryptic digestion at 37 °C overnight, the resulting peptide mixtures were extracted and vacuum-concentrated (dried) prior to MS analysis. Reconstituted peptide digests were analyzed by LC MS/MS utilizing an UltiMate 3000 UHPLC (Thermo Fisher Scientific) coupled on-line to an Orbitrap Fusion Lumos mass spectrometer (Thermo Fisher Scientific). Reverse-phase separation was performed on a 15-cm × 75-μm inner diameter Acclaim® PepMap RSLC column; peptides were eluted using a gradient of 4–25% B over 60 min at a flow rate of 300 nl/min (solvent A: 100% H_2O, 0.1% formic acid; solvent B: 100% acetonitrile, 0.1% formic acid).

Spectra for identification of glycosylated peptides were first obtained using a data-dependent acquisition method consisting of one full Fourier transform scan mass spectrum (375–1500 *m/z*, resolution of 120,000) followed by data-dependent MS/MS acquired at top speed in the linear ion trap with 30% NCE HCD for 3 s. Ions selected for MS/MS were dynamically excluded for 60 s. Raw spectrometric data were converted to MGF format using MSConvert (version 3.0.10738) and subjected to protein database searching via Batch-Tag within a developmental version of Protein Prospector (version 5.19.1, University of California, San Francisco) against bovine bOPSR (accession no. Q9BGI7). Mass tolerances for parent ions were set as ± 10 ppm and 0.1 Da, respectively. Trypsin was set as the digestive enzyme with two maximum missed cleavages allowed. Cysteine carbamidomethylation was selected as a constant modification, and protein N-terminal acetylation, methionine oxidation, and N-terminal conversion of glutamine to pyroglutamic acid were selected as variable modifications. In addition, modifications corresponding to asparagine deamidation and various glycan compositions for serine and threonine were selected as variable modifications, corresponding to *N*- and *O*-glycosylated residues. Minimum protein and peptide scores were set as 22.0 and 15.0, respectively, whereas maximum *E* values for proteins and peptides were both set to 0.01. A list of precursor ions corresponding to peptides containing the same *O*-glycosylation sites was generated for targeted sequencing for further validation. All MS/MS spectra for glycosylated peptides were further inspected manually.

Heterologous expression of hOPSG

The C terminus of hOPSG expressed in mammalian cells was truncated after residue Asp-343, whereas the hOPSG constructs expressed in Sf9 were truncated after Lys-352. All the hOPSG constructs were C-terminally tagged with the 1D4 mAB epitope (the nine C-terminal residues of bovine rhodopsin). The constructs were immunopurified with immobilized 1D4 antibody (32).

Expression, reconstitution with 11-*cis*-retinal, and purification of hOPSG and hOPSG/T4L fusion constructs in Sf9 insect cells were performed in a dark room under dim red light as described previously (22). In construct hOPSG/T4L, residues Lys-251$^{5.70}$ to Glu-257$^{6.24}$ (numbering in Ballesteros-Weinstein system (33)) of hOPSG intracellular loop 3 were replaced by T4 lysozyme. In addition, three N-terminal deletion variants of OPSG/T4L were expressed: Δ16N OPSG/T4L, Δ27N OPSG/T4L, and Δ43N OPSG/T4L (see Fig. 7*A* for sequences). Tran-

sient expressions of hOPSG in HEK293–6E cells and glycosylation-deficient HEK293SGnTI$^-$ cells were conducted by GenScript (Piscataway, NJ).

Author contributions—D. S., C. Y., L. H., and K. P. conceptualization; D. S. resources; D. S., C. Y., L. H., and K. P. data curation; D. S. and T. A. G. software; D. S., H. J., T. A. G., C. Y., and K. P. formal analysis; D. S. and H. J. investigation; D. S. visualization; D. S., H. J., T. A. G., and K. P. writing-original draft; D. S., T. A. G., and K. P. writing-review and editing; C. Y. methodology; L. H. and K. P. funding acquisition.

Acknowledgments—This work was partially carried out at the Department of Pharmacology, Case Western Reserve University, Cleveland, OH. This work was supported by a Research to Prevent Blindness (RPB) grant to the Department of Ophthalmology at the University of California, Irvine. We are grateful for the help provided by Dr. Wenyu Sun (Polgenix, Inc.). We also thank our colleagues at Case Western Reserve University who helped obtain retina samples: Drs. Les Kallestad and Tim Owen (13LGS retinas); Elliot Choi and Dr. Henri Leinonen (mouse retinas); David Peck (porcine retinas); Dr. Sahil Gulati (bovine and chicken COS/ROS); Dr. Natalia Mast (human retinas); Dr. Jianye Zhang (macaque retinas); and Philip Ropelewski (Xenopus retinas). Our thanks to Remy Zimmerman and Drs. Angele Nalbandian, Tim Kern, and Philip Kiser (University of California, Irvine) for their insightful comments on this manuscript.

References

1. Molday, R. S. (1998) Photoreceptor membrane proteins, phototransduction, and retinal degenerative diseases. The Friedenwald Lecture. *Invest. Ophthalmol. Vis. Sci.* **39,** 2491–2513 Medline
2. Pearring, J. N., Salinas, R. Y., Baker, S. A., and Arshavsky, V. Y. (2013) Protein sorting, targeting and trafficking in photoreceptor cells. *Prog. Retin. Eye Res.* **36,** 24–51 CrossRef Medline
3. Jacobs, G. H. (2015) in *Handbook of Color Psychology* (Elliott, A. J., and Franklin, A., eds) pp. 110–130, Cambridge University Press, Cambridge, UK
4. Murray, A. R., Vuong, L., Brobst, D., Fliesler, S. J., Peachey, N. S., Gorbatyuk, M. S., Naash, M. I., and Al-Ubaidi, M. R. (2015) Glycosylation of rhodopsin is necessary for its stability and incorporation into photoreceptor outer segment discs. *Hum. Mol. Genet.* **24,** 2709–2723 CrossRef Medline
5. Kaushal, S., Ridge, K. D., and Khorana, H. G. (1994) Structure and function in rhodopsin: the role of asparagine-linked glycosylation. *Proc. Natl. Acad. Sci. U.S.A.* **91,** 4024–4028 CrossRef Medline
6. Reeves, P. J., Callewaert, N., Contreras, R., and Khorana, H. G. (2002) Structure and function in rhodopsin: high-level expression of rhodopsin with restricted and homogeneous *N*-glycosylation by a tetracycline-inducible *N*-acetylglucosaminyltransferase I-negative HEK293S stable mammalian cell line. *Proc. Natl. Acad. Sci. U.S.A.* **99,** 13419–13424 CrossRef Medline
7. Hofmann, L., Alexander, N. S., Sun, W., Zhang, J., Orban, T., and Palczewski, K. (2017) Hydrogen/deuterium exchange mass spectrometry of human green opsin reveals a conserved Pro–Pro motif in extracellular loop 2 of monostable visual G protein-coupled receptors. *Biochemistry* **56,** 2338–2348 CrossRef Medline
8. Vissers, P. M., and DeGrip, W. J. (1996) Functional expression of human cone pigments using recombinant baculovirus: compatibility with histidine tagging and evidence for *N*-glycosylation. *FEBS Lett.* **396,** 26–30 CrossRef Medline
9. Gerken, T. A., Jamison, O., Perrine, C. L., Collette, J. C., Moinova, H., Ravi, L., Markowitz, S. D., Shen, W., Patel, H., and Tabak, L. A. (2011) Emerging paradigms for the initiation of mucin-type protein *O*-glycosylation by the polypeptide GalNAc transferase family of glycosyltransferases. *J. Biol. Chem.* **286,** 14493–14507 CrossRef Medline
10. Bennett, E. P., Mandel, U., Clausen, H., Gerken, T. A., Fritz, T. A., and Tabak, L. A. (2012) Control of mucin-type *O*-glycosylation: a classification of the polypeptide GalNAc-transferase gene family. *Glycobiology* **22,** 736–756 CrossRef Medline
11. Goth, C. K., Vakhrushev, S. Y., Joshi, H. J., Clausen, H., and Schjoldager, K. T. (2018) Fine-tuning limited proteolysis: a major role for regulated site-specific *O*-glycosylation. *Trends Biochem. Sci.* **43,** 269–284 CrossRef Medline
12. Steentoft, C., Vakhrushev, S. Y., Joshi, H. J., Kong, Y., Vester-Christensen, M. B., Schjoldager, K. T., Lavrsen, K., Dabelsteen, S., Pedersen, N. B., Marcos-Silva, L., Gupta, R., Bennett, E. P., Mandel, U., Brunak, S., Wandall, H. H., *et al.* (2013) Precision mapping of the human *O*-GalNAc glycoproteome through SimpleCell technology. *EMBO J.* **32,** 1478–1488 CrossRef Medline
13. Gerken, T. A., Raman, J., Fritz, T. A., and Jamison, O. (2006) Identification of common and unique peptide substrate preferences for the UDP-GalNAc:polypeptide α-*N*-acetylgalactosaminyltransferases T1 and T2 derived from oriented random peptide substrates. *J. Biol. Chem.* **281,** 32403–32416 CrossRef Medline
14. Kong, Y., Joshi, H. J., Schjoldager, K. T., Madsen, T. D., Gerken, T. A., Vester-Christensen, M. B., Wandall, H. H., Bennett, E. P., Levery, S. B., Vakhrushev, S. Y., and Clausen, H. (2015) Probing polypeptide GalNAc-transferase isoform substrate specificities by *in vitro* analysis. *Glycobiology* **25,** 55–65 CrossRef Medline
15. Jacobs, G. H., Fisher, S. K., Anderson, D. H., and Silverman, M. S. (1976) Scotopic and photopic vision in the California ground squirrel: physiological and anatomical evidence. *J. Comp. Neurol.* **165,** 209–227 CrossRef Medline
16. Papermaster, D. S. (1982) Preparation of retinal rod outer segments. *Methods Enzymol.* **81,** 48–52 CrossRef Medline
17. Jones, B. W., Kondo, M., Terasaki, H., Watt, C. B., Rapp, K., Anderson, J., Lin, Y., Shaw, M. V., Yang, J. H., and Marc, R. E. (2011) Retinal remodeling in the Tg P347L rabbit, a large-eye model of retinal degeneration. *J. Comp. Neurol.* **519,** 2713–2733 CrossRef Medline
18. Tachibana, K., Nakamura, S., Wang, H., Iwasaki, H., Tachibana, K., Maebara, K., Cheng, L., Hirabayashi, J., and Narimatsu, H. (2006) Elucidation of binding specificity of Jacalin toward *O*-glycosylated peptides: quantitative analysis by frontal affinity chromatography. *Glycobiology* **16,** 46–53 CrossRef Medline
19. Palczewski, K., Kumasaka, T., Hori, T., Behnke, C. A., Motoshima, H., Fox, B. A., Le Trong, I., Teller, D. C., Okada, T., Stenkamp, R. E., Yamamoto, M., and Miyano, M. (2000) Crystal structure of rhodopsin: a G protein-coupled receptor. *Science* **289,** 739–745 CrossRef Medline
20. Bourne, H. R., and Meng, E. C. (2000) Structure. Rhodopsin sees the light. *Science* **289,** 733–734 CrossRef Medline
21. Stenkamp, R. E., Filipek, S., Driessen, C. A., Teller, D. C., and Palczewski, K. (2002) Crystal structure of rhodopsin: a template for cone visual pigments and other G protein-coupled receptors. *Biochim. Biophys. Acta* **1565,** 168–182 CrossRef Medline
22. Owen, T. S., Salom, D., Sun, W., and Palczewski, K. (2018) Increasing the stability of recombinant human green cone pigment. *Biochemistry* **57,** 1022–1030 CrossRef Medline
23. Alexander, N. S., Katayama, K., Sun, W., Salom, D., Gulati, S., Zhang, J., Mogi, M., Palczewski, K., and Jastrzebska, B. (2017) Complex binding pathways determine the regeneration of mammalian green cone opsin with a locked retinal analogue. *J. Biol. Chem.* **292,** 10983–10997 CrossRef Medline
24. Lopez, M., Tetaert, D., Juliant, S., Gazon, M., Cerutti, M., Verbert, A., and Delannoy, P. (1999) *O*-Glycosylation potential of lepidopteran insect cell lines. *Biochim. Biophys. Acta* **1427,** 49–61 CrossRef Medline
25. Goth, C. K., Tuhkanen, H. E., Khan, H., Lackman, J. J., Wang, S., Narimatsu, Y., Hansen, L. H., Overall, C. M., Clausen, H., Schjoldager, K. T., and Petäjä-Repo, U. E. (2017) Site-specific *O*-glycosylation by polypeptide *N*-acetylgalactosaminyltransferase 2 (GalNAc-transferase T2) co-regulates β1-adrenergic receptor N-terminal cleavage. *J. Biol. Chem.* **292,** 4714–4726 CrossRef Medline

26. Lackman, J. J., Goth, C. K., Halim, A., Vakhrushev, S. Y., Clausen, H., and Petäjä-Repo, U. E. (2018) Site-specific *O*-glycosylation of N-terminal serine residues by polypeptide GalNAc-transferase 2 modulates human δ-opioid receptor turnover at the plasma membrane. *Cell. Signal.* **42,** 184–193 CrossRef Medline
27. Opefi, C. A., South, K., Reynolds, C. A., Smith, S. O., and Reeves, P. J. (2013) Retinitis pigmentosa mutants provide insight into the role of the N-terminal cap in rhodopsin folding, structure, and function. *J. Biol. Chem.* **288,** 33912–33926 CrossRef Medline
28. Cummings, R. D., Liu, F. T., and Vasta, G. R. (2015) in *Essentials of Glycobiology* (Varki, A., Cummings, R. D., Esko, J. D., Stanley, P., Hart, G. W., Aebi, M., Darvill, A. G., Kinoshita, T., Packer, N. H., Prestegard, J. H., Schnaar, R. L., and Seeberger, P. H., eds) pp. 469–480, Cold Spring Harbor Laboratory Press, Cold Spring Harbor, NY
29. Craig, S. E., Thummel, R., Ahmed, H., Vasta, G. R., Hyde, D. R., and Hitchcock, P. F. (2010) The zebrafish galectin Drgal1–L2 is expressed by proliferating Muller glia and photoreceptor progenitors and regulates the regeneration of rod photoreceptors. *Invest. Ophthalmol. Vis. Sci.* **51,** 3244–3252 CrossRef Medline
30. Nakagawa, M., Miyamoto, T., Kusakabe, R., Takasaki, S., Takao, T., Shichida, Y., and Tsuda, M. (2001) *O*-Glycosylation of G-protein-coupled receptor, octopus rhodopsin. Direct analysis by FAB mass spectrometry. *FEBS Lett.* **496,** 19–24 CrossRef Medline
31. Steiner, L. (1988) in *Antibodies: A Laboratory Manual* (Harlow, E., and Lane, D., eds) p. 726, Cold Spring Harbor Laboratory Press, Cold Spring Harbor, New York
32. Salom, D., Le Trong, I., Pohl, E., Ballesteros, J. A., Stenkamp, R. E., Palczewski, K., and Lodowski, D. T. (2006) Improvements in G protein-coupled receptor purification yield light stable rhodopsin crystals. *J. Struct. Biol.* **156,** 497–504 CrossRef Medline
33. Visiers, I., Ballesteros, J. A., and Weinstein, H. (2002) Three-dimensional representations of G protein-coupled receptor structures and mechanisms. *Methods Enzymol.* **343,** 329–371 CrossRef Medline